Surface-State Stark Shift in a Scanning Tunneling Microscope

L. Limot,[1] T. Maroutian,[1] P. Johansson,[2] and R. Berndt[1]

[1]*Institut für Experimentelle und Angewandte Physik, Christian-Albrechts-Universität zu Kiel, D-24098 Kiel, Germany*
[2]*Department of Natural Sciences, University of Örebro, S-70182, Örebro, Sweden*

(Received 29 January 2003; published 3 November 2003)

We report a quantitative low-temperature scanning tunneling spectroscopy (STS) study on the Ag(111) surface state over an unprecedented range of currents (50 pA to 6 μA) through which we can tune the electric field in the tunnel junction of the microscope. We show that in STS a sizable Stark effect causes a shift of the surface-state binding energy E_0. Data taken are reproduced by a one-dimensional potential model calculation, and are found to yield a Stark-free energy E_0 in agreement with recent state-of-the-art photoemission spectroscopy measurements.

DOI: 10.1103/PhysRevLett.91.196801 PACS numbers: 73.20.–r, 68.37.Ef

Surface states have been investigated intensely for over two decades of surface science. These states, which are trapped between the surface barrier potential and a band gap in the crystal, are an experimental realization of a quasi-two-dimensional electron gas with a characteristic dispersion of $E(k) - E_0 \propto k^2$, where E_0 is the lower edge of the energy band. Scanning tunneling microscopy (STM) and scanning tunneling spectroscopy (STS) have provided a new way to study surface states through local measurements performed on the atomic scale. The first imaging of Shockley surface states on the (111) facet of the noble metals Ag, Cu, and Au has motivated a great deal of STM and STS studies on these systems [1]. Since then, many aspects have been elucidated such as surface-state-mediated interactions [2], and lateral confinement to nanocavities [3]. The lifetime τ of these states at E_0, as determined by STS [4–6], also agrees remarkably well with recent state-of-the-art angle-resolved photoemission spectroscopy (PES) measurements [7]. Despite this success, a worrying discrepancy between STS and PES still subsists in noble metals concerning E_0, as E_0(STS) is found to lie lower than E_0(PES) typically by -5 to -20 meV [4,7].

This last point is still an open question. A possible explanation would be that unlike STS, where the local character of the measurement allows to access a defect-free region of the surface, a PES measurement is defect sensitive as it integrates over a large sample area of about 1 mm^2. And defects should, in principle, shift E_0(PES) upwards in energy [8]. However defects also broaden the PES line width [Γ(PES) $= \hbar/\tau$], and the recent agreement found for τ between STS and PES appears to invalidate this scenario.

In this Letter, we present STS measurements on the surface state of Ag(111) which elucidate this discrepancy. The presence of an electric field between the STM tip and the sample surface is known to produce a Stark shift in the STS spectra of field emission resonance states [9], or a more dramatic effect such as band bending in semiconductors [10]. With this in mind, we have tracked down the influence of the electric field on the STS spectrum of the Ag(111) surface state. The tunneling current I in a STM junction can be written as

$$I \propto \exp(-1.025\sqrt{\phi}d), \tag{1}$$

where ϕ is the apparent barrier height and d the tip-surface distance; hence, the electric field ($\sim 1/d$) can be conveniently tuned through I. By spanning I over 50 pA–6 μA and recording concomitantly the surface-state spectrum, we establish on an experimental basis the existence of a downward Stark shift in E_0(STS). We also provide a one-dimensional model which describes the Stark contribution. We extract the Stark-shift-free energy E_0 of Ag(111) and find it to agree with the PES value (where no electric field is present).

The Ag(111) surface was cleaned by Ar^+ sputter/anneal cycles, and the measurements were performed in a custom-built ultrahigh vacuum STM operating at a temperature of 4.6 K, using electrochemically etched W tips, further treated *in situ* by indentations into the surface. Spectroscopy of the differential conductance dI/dV versus the sample voltage V was performed by opening the feedback loop at $V = 100$ mV in the center of impurity- and step-free regions of the surface (≥ 400 nm^2). A lock-in detection amplifier was employed to record the dI/dV (ac voltage modulation was 1 mV rms and $\sim$1–10 kHz, and a single spectrum was acquired in $\sim$3–10 s). The dependency of the dI/dV spectrum on d is probed through Eq. (1) by varying I.

Figure 1 summarizes the essential experimental findings. The sharp steplike rise of the conductance shown in Fig. 1(a) for $I = 1$ nA allows one to determine the low edge of the energy band of the Ag(111) surface state—at $E_0 = -66.7(5)$ meV in Fig. 1(a), in agreement with previous STS studies [4], but lower than E_0 (PES) $= -63(1)$ meV [7]. In contrast, from the width Δ of the onset we extract Γ(STS) $= 6.4(5)$ meV [5], in agreement with Γ(PES) $= 6.0(5)$ meV. When increasing I, a sizable shift of E_0 occurs. In typical dI/dV spectra [Fig. 1(b)] the surface state onset shifts downward in energy with no appreciable broadening as I increases from a pA range to

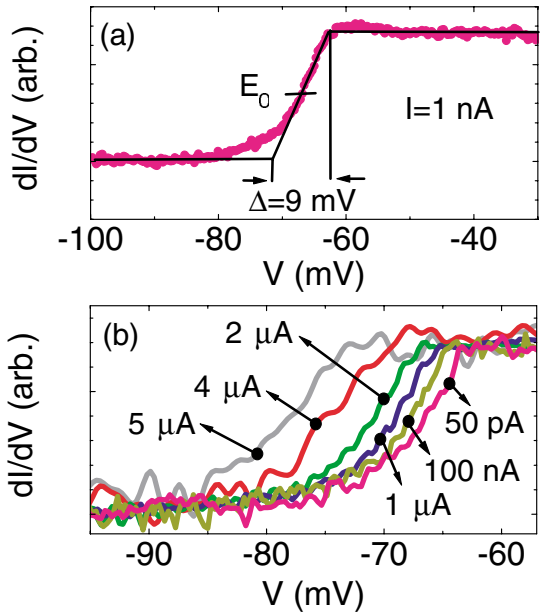

FIG. 1 (color online). (a) Typical dI/dV spectrum taken on Ag(111) ($T = 4.6$ K). The feedback loop was opened at $I = 1$ nA and $V = 100$ mV. A geometrical analysis is used to determine E_0 and the width Δ of the surface state [4,5]. (b) Downward shift of E_0 when I is increased. All spectra are averages of at least five single spectra from varying sample locations and tips; the spectra were renormalized to match the conductance of the 50 pA spectrum.

a μA range. At $I = 6$ μA, the highest current where we could perform reliable spectroscopy, E_0 has shifted by -20% with respect to $I = 50$ pA. The dependence of E_0 on I, i.e., on the tip-surface distance, is the major finding of this Letter.

Figure 2 presents a quantitative evaluation of E_0 for all tunneling currents investigated. Two distinct regimes are found for the band edge shift—also directly visible on the spectra of Fig. 1(b): typically 50 pA $\leq I \leq 1$ μA over which E_0 decreases by -4 meV, and 2 μA $< I \leq 6\mu$A where the shift of E_0 is more pronounced (-10 meV).

Care was taken to systematically survey the tip and the surface status during spectrum acquisition. We proceeded as follows: (i) for a given tip preparation a $I = 1$ nA spectrum is acquired and E_0 is evaluated following the geometrical analysis detailed in Fig. 1(a), (ii) I is then set to the value of interest and a spectrum is recorded, (iii) the tip and the surface status are checked through a final 1 nA spectrum. To minimize errors in the evaluation of the shift, each spectrum acquired in step (ii) was fitted to the 1 nA spectrum of step (i) in order to determine E_0. For all the data reported in this Letter, no change was discernible in the spectra acquired in step (i) and in step (iii), meaning that neither a tip modification nor a tip-induced damage of the surface occurred when acquiring spectra in the 50 pA–6 μA range. This conclusion also agrees with the absence of any modification in the surface images acquired before step (i) and after step (iii).

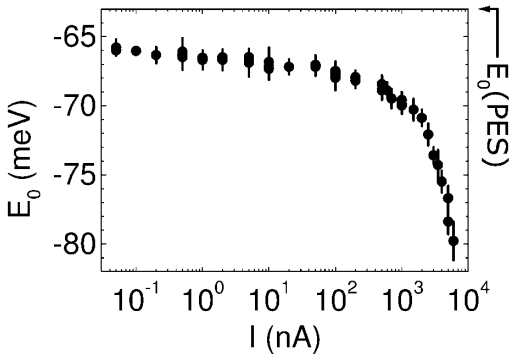

FIG. 2. E_0 vs I. The arrow indicates the PES value of E_0 [7].

Before going any further, a remark concerning the experimental setup is necessary. Given the unusually wide range of the tunneling resistances R employed in this study (from 20 kΩ to 2 GΩ), the possibility of a voltage drop at the input impedance R_{in} of the current preamplifier has to be considered. It would decrease the bias voltage at the tunneling junction by $(1 + R_{\text{in}}/R)^{-1}$ thus producing a sizable R-dependent, i.e., I-dependent, shift of the spectrum when $R \sim R_{\text{in}}$. With the variable gain current preamplifier employed *this does not occur*, since $R_{\text{in}}/R \approx 0.3\%$ at most (this condition is met for both dc and ac signals at the modulation frequencies used). To highlight this point, Fig. 3(a) displays two spectra acquired at 10 nA but with gains of 10^7 and 10^8 V/A for which $R_{\text{in}}/R = 0.02\%$ and $R_{\text{in}}/R = 0.1\%$, respectively. As expected, their difference is a flat line over the entire voltage range [Fig. 3(b)], even in the onset region where a shift artifact would produce a spike. This is also true for pairs of spectra acquired at 1 nA, 100 nA, and 1 μA at different gains. In conclusion, no relevant voltage drop is present in our setup at the tunneling currents of interest.

In order to express the dependency of E_0 on the tip-surface distance, we measured the variation of I over 20 pA $-$ 6 μA while approaching, with the feedback loop open, the tip towards the surface by ≈ 6 Å. The recorded currents follow an exponential behavior up to $\approx$ 2 μA, from which we extract through Eq. (1) an apparent barrier height of $\phi = 4.0(2)$ eV, typical for noble metals [11]. In contrast, for $I \gtrsim 2$ μA, I increases faster than expected. It is well known from break junction experiments [12] that this signals that the junction is no longer in a tunneling regime, rather in a contact regime where, as we discuss below, important modifications of the tip and the surface morphologies occur.

Our results are summarized in Fig. 4, where E_0 is now plotted versus the tip-surface displacement. As shown, the negative Stark shift of E_0 can be tuned by approaching or retracting the tip from the surface. To gain further insight, we propose a model which describes the experimental data and enables extrapolation to the zero-field properties of the surface state. We first detail some aspects of the model and then discuss the calculation in light of our data.

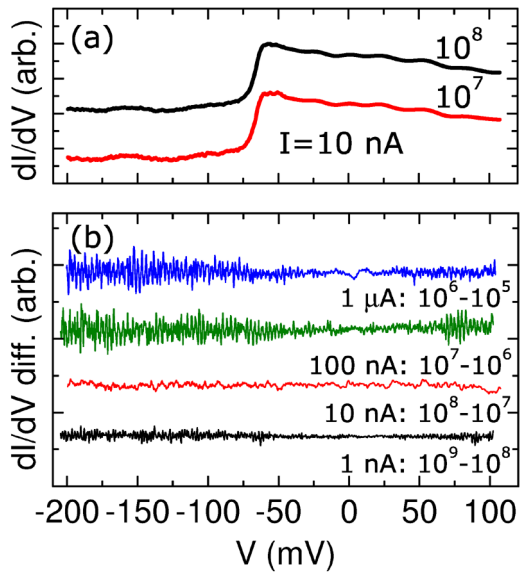

FIG. 3 (color online). (a) dI/dV spectra acquired at 10 nA, 100 mV, with a 10^7 and a 10^8 V/A gain of the current preamplifier. (b) Differences between pairs of spectra acquired at the same currents (1 nA, 10 nA, 100 nA, and 1 μA) but with different gains. Gains range from 10^5 to 10^9 V/A with R_{in} = 50 Ω, 60 Ω, 150 Ω, 1 kΩ, and 10 kΩ, respectively. Spectra are shifted vertically for clarity.

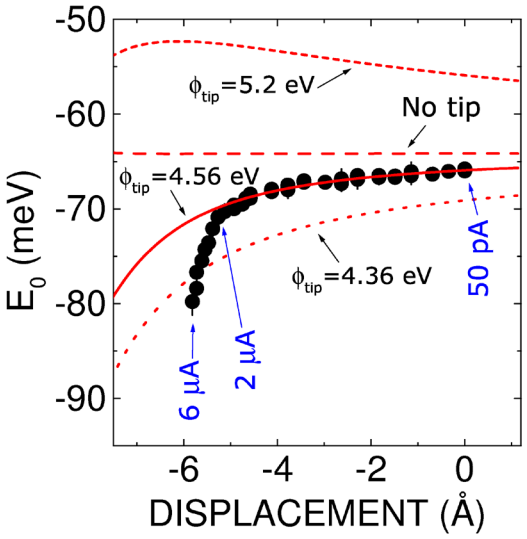

FIG. 4 (color online). E_0 versus tip-surface distance. Since experimentally we only probe a displacement of the tip towards the surface, the calculated curves were shifted horizontally to match the data (the origin is arbitrarily fixed at 50 pA). Lines show calculated results for tip work functions ϕ_{tip}: 4.56 eV (solid line), 4.36 eV (dotted line), 5.2 eV (short dashed line), and in absence of the tip (dashed line). Also shown, the boundaries to the 2–6 μA region.

The Ag(111) surface-state electrons are modeled with the one-dimensional potential proposed by Chulkov *et al.* [13]. This potential is periodic in the bulk ($z < 0$), has a potential well just outside the surface ($0 < z < z_1$), then decays exponentially towards the vacuum ($z_1 < z < z_{im}$) to finally cross over to a long-range image potential ($z > z_{im}$). To take into account the presence of the tip at $z \geq z_{tip}$, we added to the potential the linear contribution of the voltage bias V between tip and surface, as well as the difference between the work functions of the tip (ϕ_{tip}) and the surface (ϕ_{samp}) to include the contact potential. Furthermore, we modified the shape of the image potential to account for multiple images in the tip and the surface. This yields

$$V(z) = 2V_{111}\cos gz, \qquad z < 0,$$
$$V(z) = V_{20} + V_2\cos\beta z, \qquad 0 < z < z_1,$$
$$V(z) = V_{lin}(z) + V_3 e^{-\alpha(z-z_1)}, \qquad z_1 < z < z_{im},$$
$$V(z) = V_{lin}(z) - V_{im}(z), \qquad z_{im} < z < z_{tip},$$

where

$$V_{lin}(z) = E_F + s(eV + \phi_{tip}) + (1-s)\phi_{samp},$$

where E_F is the surface Fermi energy, $s = (z - z_1)/(z_{tip} - z_1)$, and

$$V_{im}(z) = [1 - e^{-\lambda(z-z_{im})}]\frac{e^2[2\Psi(1) - \Psi(\zeta) - \Psi(1-\zeta)]}{16\pi\epsilon_0(z_{im}^{tip} - z_{im})},$$

with $\zeta = (z - z_{im})/(z_{im}^{tip} - z_{im})$ and Ψ is the digamma function. The parameters V_{111}, g, V_{20}, V_2, β, and $z_1 = 5\pi/4\beta$ describing the potential in the absence of the tip are fixed to their corresponding values of Ref. [13]. The remaining parameters V_3, α, λ, and z_{im} and z_{im}^{tip}, were fixed by requiring the potential and its derivative to be continuous everywhere, except at $z = z_{tip}$ for the derivative. The energy of the surface state at a given tip-surface distance was calculated by searching for the corresponding maximum in the transmission probability of the tunneling electrons (an imaginary part was introduced in the potential between $0 \leq z \leq z_1$ to mimic the inelastic scattering).

The calculation performed with the Ag(111) work function $\phi_{samp} = \phi_{tip} = 4.56$ eV for both tip and surface (solid line in Fig. 4) reproduces the data up to $I \approx 2$ μA [14], where a strong discrepancy is observed. We first focus on the $I \lesssim 2$ μA region were the model works. To probe the influence of the contact potential, we performed calculations with different values for ϕ_{tip}: for a pure W tip ($\phi_{tip} = 5.20$ eV, short dashed line in Fig. 4), and for a Ag coated tip with a high density of surface defects ($\phi_{tip} = 4.36$ eV, dotted line in Fig. 4). The contact potential yields, in the former case, a positive Stark shift, whereas the latter increases the downward shift. As shown, neither of them reproduces the experimental behavior as well as the calculation with $\phi_{tip} = 4.56$ eV does. Although we cannot fully exclude a contribution from the contact potential, from these considerations we conclude that, for the tips used, it must bear a negligible contribution to the Stark effect. We note also that since the data was obtained with a variety of tips, the highly

reproducible shift observed indicates that our *in situ* tip preparation must lead to similar tip apices. In conclusion, on the basis of our model, at the largest tip-surface distances shown, the Stark effect is mainly produced by the bias and by the lowering of the image potential compared with the case of an isolated surface, with a 2 to 1 ratio between the two. However, as the distance is reduced the lowering of the image potential is increasingly stronger and eventually governs the Stark effect.

Now we discuss the asymptotic behavior of the Stark effect. As the tip is retracted, the Stark contribution decreases towards the nonperturbed binding energy which is calculated by suppressing the presence of the tip in our model. It yields a constant value of $E_0 = -64$ meV with tip-surface distance (dashed line in Fig. 4), in agreement with the Stark-free PES value for Ag(111). Figure 4 shows that the Stark effect cannot be suppressed, as the tip would have to be retracted well beyond the lowest tunneling currents experimentally accessible, typically in the pA range. For Ag(111) the Stark shift results then, at best, in a ~4% error in the evaluation of E_0.

We now turn to the $I \gtrsim 2\ \mu$A region where our model calculation no longer reproduces the experimental data. The comparison between the two indicates that the actual electric field in the junction is stronger than the one predicted in our model calculation. Since in the model the tip and surface morphologies are assumed to be constant at all tunneling currents, we hint that in the $I \gtrsim 2\ \mu$A range, i.e., $R \lesssim 50\ \mathrm{k}\Omega$, the tip and the surface deform to yield a stronger electric field. This deformation is reversible, since the spectra acquired at $I = 1$ nA prior and after ramping the current to $I \gtrsim 2\ \mu$A (three-step procedure described earlier) did not yield any substantial differences. This picture agrees with calculations performed for Au(100) [11], which indicate that the tip and the surface undergo an elastic deformation, i.e., they stretch towards each other, because of attractive adhesive forces acting at $R \lesssim 100\ \mathrm{k}\Omega$. In particular, this is predicted to result in a deviation from the exponential behavior of Eq. (1), which we do indeed observe in the I versus displacement measurements at $I \gtrsim 2\ \mu$A.

To summarize, in STS a downward shift of the binding energy of the Ag(111) surface state occurs when decreasing tip-surface distance. A model calculation explains this observation in terms of a Stark shift produced by the bias and by the lowering of the image potential compared to an isolated surface. We extract a nonperturbed value of -64 meV for E_0 in agreement with PES measurements, and conclude that a possible positive shift of E_0(PES) in Ref. [7] due to surface defects is negligible. Finally, for tunneling resistances $R \lesssim 50\ \mathrm{k}\Omega$, an enhanced shift is observed, which we assign to an elastic deformation of the tip-surface morphology. These results, supported by our recent observation of a Stark effect for other noble metal surface states and for the Ag/Ag(111) adatom [15], suggest that STS data require a thorough quantification of the Stark effect when striving for high energy resolution, especially for states whose wave functions have large decay lengths into vacuum.

We gratefully acknowledge G. Hoffmann whose results for Na/Cu(111) motivated this work, and J. Kröger, J. Kuntze, and S. Crampin for fruitful discussions. L. L., T. M., and R. B. thank the Deutsche Forschungsgemeinschaft for financial support, and P. J. thanks the Swedish Natural Science Research Council (VR).

[1] L. C. Davis, M. P. Everson, R. C. Jaklevic, and W. Shen, Phys. Rev. B **43**, 3821 (1991); Y. Hasegawa and Ph. Avouris, Phys. Rev. Lett. **71**, 1071 (1993); M. F. Crommie, C. P. Lutz, and D. M. Eigler, Nature (London) **363**, 524 (1993).

[2] J. Repp, F. Moresco, G. Meyer, K.-H. Rieder, P. Hyldgaard, and M. Persson, Phys. Rev. Lett. **85**, 2981 (2000); N. Knorr, H. Brune, M. Epple, A. Hirstein, M. A. Schneider, and K. Kern, Phys. Rev. B **65**, 115420 (2002).

[3] E. J. Heller, M. F. Crommie, C. P. Lutz, and D. M. Eigler, Nature (London) **369**, 464 (1994); J. Li, W.-D. Schneider, R. Berndt, and S. Crampin, Phys. Rev. Lett. **80**, 3332 (1998); K.-F. Braun and K.-H. Rieder, Phys. Rev. Lett. **88**, 96 801 (2002).

[4] J. Kliewer, R. Berndt, E. V. Chulkov, V. M. Silkin, P. M. Echenique, and S. Crampin, Science **288**, 1399 (2000).

[5] J. Li, W.-D. Schneider, R. Berndt, O. R. Bryant, and S. Crampin, Phys. Rev. Lett. **81**, 4464 (1998).

[6] L. Bürgi, O. Jeandupeux, H. Brune, and K. Kern, Phys. Rev. Lett. **82**, 4516 (1999).

[7] F. Reinert, G. Nicolay, S. Schmidt, D. Ehm, and S. Hüfner, Phys. Rev. B **63**, 115415 (2001).

[8] See, for example, F. Theilmann, R. Matzdorf, G. Meister, and A. Goldmann, Phys. Rev. B **56**, 3632 (1997).

[9] R. S. Becker, J. A. Golovchenko, and B. S. Swartzentruber, Phys. Rev. Lett. **55**, 987 (1985); G. Binnig, K. H. Frank, H. Fuchs, N. Garcia, B. Reihl, H. Rohrer, F. Salvan, and A. R. Williams, *ibid.* **55**, 991 (1985).

[10] M. McEllistrem, G. Haase, D. Chen, and R. J. Hamers, Phys. Rev. Lett. **70**, 2471 (1993).

[11] L. Olesen, M. Brandbyge, M. R. Sørensen, K. W. Jacobsen, E. Lægsgaard, I. Stensgaard, and F. Besenbacher, Phys. Rev. Lett. **76**, 1485 (1996).

[12] J. M. Krans, C. J. Muller, I. K. Yanson, Th. C. M. Govaert, R. Hesper, and J. M. van Ruitenbeek, Phys. Rev. B **48**, 14 721 (1993).

[13] E. V. Chulkov, V. M. Silkin, and P. M. Echenique, Surf. Sci. **437**, 330 (1999).

[14] The Fermi energy is fixed to $E_F = 5.085$ eV so that the calculated curve with $\phi_{\mathrm{samp}} = \phi_{\mathrm{tip}} = 4.56$ eV matches the experimental data. This procedure we employ to determine E_F differs from the approach of Ref. [13].

[15] J. Kröger, L. Limot, P. Johansson, and R. Berndt (unpublished).